Control and Fuzzy Logic Supervision of a Wind Power System With Battery/Supercapacitor Hybrid Energy Storage

Youssef KRIM[1], Dhaker ABBES[2], Saber KRIM[1] and Mohamed Faouzi MIMOUNI[1]
[1]National Engineering School of Monastir, Electrical Engineering Department, 5019, University of Monastir–Tunisia
Krim_enim@hotmail.com, saber.krim@polytecsousse.tn, MFaouzi.Mimouni@enim.rnu.tn
[2]Laboratory of Electrical Engineering and Power Electronics of Lille (L2EP), Ecole des Hautes Etudes d'Ingénieur (HEI)
Yncrea Hauts-de-France. 13, rue de Toul, F-59046 Lille, France
dhaker.abbes@yncrea.fr

***Abstract*— In this paper, we propose a control and fuzzy logic power management supervisor for a grid-connected wind power system associated with Hybrid Energy Storage (HES) made up of Batteries (BT) and Supercapacitor (SC). Batteries are used to meet the energy requirements of a long-term, while SC is used to meet the demand for instant power. The SC can act as a buffer against large magnitudes and rapid fluctuations of power. The PMS is developed to manage the energy flows between the storage devices by maintaining these State Of Charge (SOC) into acceptable levels and establishes the priority order between them. The main objective of this work is the combination of two storage technologies with fuzzy logic supervision. It aims to meet the expectations of various production scenarios for a wind generator, to keep stable the DC bus voltage, and to participate in ancillary services such as : respecting a production program, supporting the grid and optimizing storage elements lifespan. Simulation results prove the efficiency of proposed power control and supervision strategy.**

Keywords*— *Wind turbine; Hybrid storage system; Power management supervisor; Fuzzy logic.

I. INTRODUCTION

Batteries (BT) are more and more used for grid-connected wind power systems [1, 2]. They are used to fulfill the power mismatch between wind power production and power demanded by load and also by system services, if the wind generator has ancillary services such as grid stability [3]. They have a high energy density but a low power density. Their lifetime expressed in the number of charge-discharge cycles is relatively limited due to the high variation of the power demanded by system services and load [4]. However, the system performance can be improved by using a supercapacitor (SC) that can also generate an active power [5]. SC energy storage is well suited for short-term storage systems, which are generally sufficient to improve the electrical power quality [6], to handle situations such as wind gust or sudden load variations which may exist for a few seconds or even longer [7], and to increase the penetration of wind generators into the power system. For this reason, SC which has a bigger power density can be used in a complementary way with BT.

In the literature, hybrid battery–supercapacitor energy storage was first explored as an alternative to the traditional battery system when subjected to pulsed loads in digital communication applications [8], and is now popularly applied in electric vehicles since they have frequent motor startups and braking events. The addition of the supercapacitor has the potential to reduce the size and improve battery life [9]. The Hybrid Energy Storage (HES) is also being considered for standalone renewable energy applications [10], as such battery–supercapacitor combinations result in better reliability and a longer battery life. In this work, HES is suggested for renewable distributed generator operating in standalone mode for supplying loads and grid connected mode for ancillary services (ensure the grid stability). Thereby, complementarities in terms of available instantaneous power and quantity of stored energy will increase the performance of renewable production system.

An optimal energy management strategy for HES is essential for managing the power flows of the BT and SC. In the event of overcharge or excess discharge, the HES must be protected to ensure safe operation. Therefore, the developed HES may improve BT lifespan as SC can act as a buffer against rapid fluctuations in power [11]. Reduction of rapid fluctuations on battery minimizes its heating and internal losses [12]. In references [13] and [14], a Rule Based Controller (RBC) and Filtration Based Controller (FBC) are implemented respectively to control a renewable power generation with HES. Despite RBC and FBC are simple to exploit, they are not well adapted for complex systems with many objectives (load satisfaction, storage supervision, frequency support, load satisfaction, improving batteries lifespan, CO2 reduction, etc.) [15]. Furthermore, a Rule-based energy management is suggested to manage the energy flows between the storage devices [16]. It is easily developed and is able to operate quite reliably. But it's not well adapted for complex systems. For example, if the wind generator has to operate at different modes (according to the variation of the power demanded by the load and the grid) and the energy management strategy considers further information about the energy storage system (available energy, degradation approach, power/energy demand, etc.), rules development becomes complex due to the increase of variables and cases to evaluate.

For this way, a fuzzy logic-based algorithm is proposed to solve the energy management problem and the energy distribution between the batteries and SC. However, the Fuzzy Logic

Supervisor (FLS) does not require complex mathematical models as used in classic control and represents it based on the human reasoning.

In this context, the aforementioned paper proposes a control and FLS for a grid-connected wind power system with hybrid battery-supercapacitors storage. It is used to ensure the continuous supply of the load by maintaining the State Of Charge (SOC) of the SC (U_{sc}(V)) and the SOC of the batteries (SOC_{bat}(%)) at acceptable levels to avoid the damaging of batteries and SC. Thus, this paper is organized as follows: The first section focus on the modeling and control of the considered wind power system. This control strategy has two main parts. The first one is the vector control of the Permanent-Magnet Synchronous Generator (PMSG) to allow the maximum power point tracking (MPPT) via a rectifier and the second one concerns DC bus voltage control. In the second section, a FLS is implemented. It is successfully applied for whole system energy management. Finally, simulation results are presented. They illustrate the robustness of the proposed power control and management strategy that ensure safe operation of the system in different scenarios.

II. Modeling and Control of Wind Distributed Generator

Figure 1 presents a synopsis of the considered Renewable Distributed Generation (RDG) which is composed by a wind power system associated with BT/SC HES. This RDG is connected with variable loads and to a fluctuating grid.

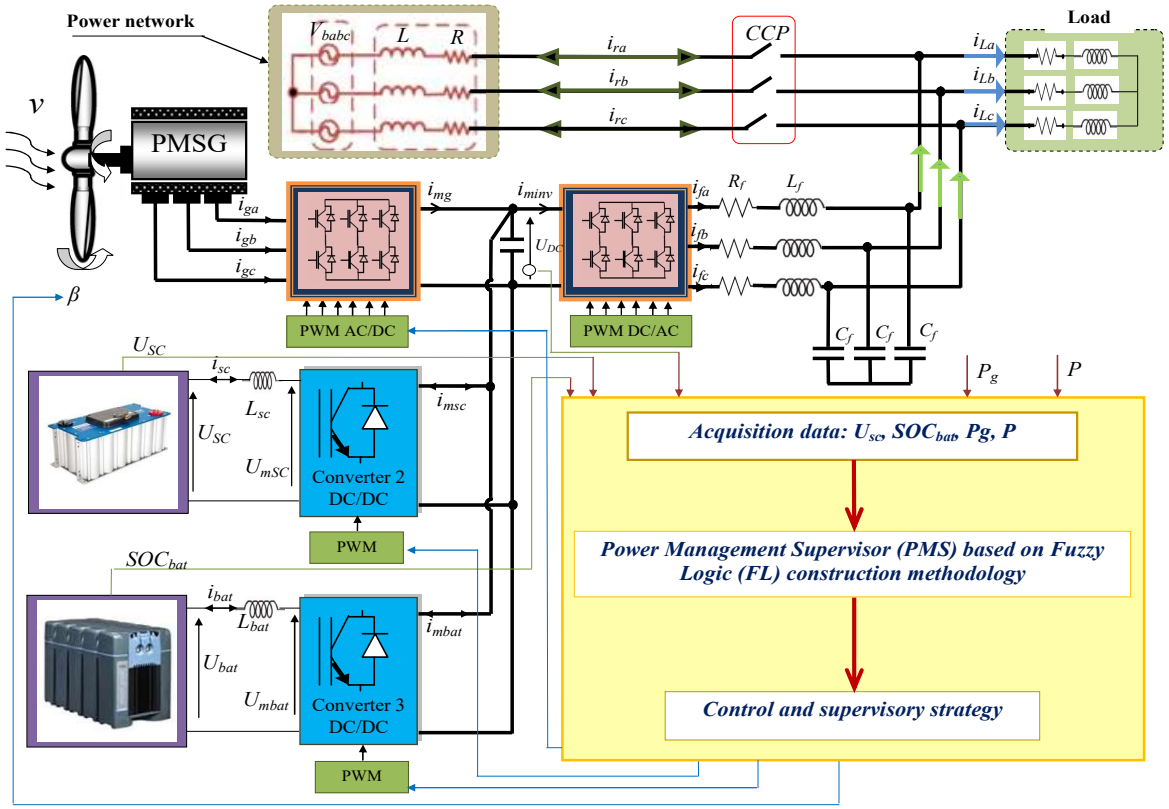

Fig. 1. Structure of studied system

A. Modeling and control of the wind generator

The wind energy production P_w (W) is expressed as a function of the instantaneous wind speed v and the area S swept by the blades [17]:

$$P_w = \frac{1}{2}\rho S v^3 C_p \tag{1}$$

where ρ is the air density.

The power coefficient C_p is a function of the ratio speed λ and a pitch angle β [18]:

$$\begin{cases} C_p(\lambda,\beta) = 0.5179\left(98\lambda_i - 0.4\beta + 5\right)e^{-21\lambda_i} + 0.068\lambda \\ \lambda = \dfrac{R\Omega_m}{v} \end{cases} \tag{2}$$

with

$$\lambda_i = \frac{1}{\dfrac{1}{\lambda + 0.089} - \dfrac{0.035}{\beta^3 + 1}} \tag{3}$$

where R(m) is the blade radius.

In this work, The PMSG is classically modeled in the d-q reference frame by the following equations [19]:

$$\begin{cases} V_{gd} = R_s i_{gd} + L_s \dfrac{di_{gd}}{dt} - p\Omega_m L_s i_{gq} \\ V_{gq} = R_s i_{gq} + L_s \dfrac{di_{gq}}{dt} + p\Omega_m L_s i_{gq} + p\Omega_m \phi_m \end{cases} \tag{4}$$

$$T_{em} = p i_{gq} \phi_m \tag{5}$$

where R_s (Ω) is the stator winding resistance, ϕ_m (Wb) represents the magnet flux, L_s (H) is the stator winding inductance,

i_{gd} and i_{gq} are the direct and quadratic stator currents, V_{gd} and V_{gq} are the direct and quadratic stator voltages, p is the number of pole pairs and Ω_m (rad/s) is the mechanical speed of the PMSG.

Figure 2 shows the control strategy of the wind generator. This strategy is based on the vector control applied to PMSG to extract maximum power. The principle of this control is to impose a direct current reference i^*_{gd} equal to zero and a quadratic current reference i^*_{gq} proportional to electromagnetic torque reference given by the MPPT algorithm as follows:

$$i^*_{gd} = 0; i^*_{gq} = \frac{T_{em_{MPPT}}}{p\phi_m} \tag{6}$$

Electromagnetic torque reference "T_{emMPPT}(N.m)" is determined by the MPPT strategy as follows [20]:

$$T_{em_{MPPT}} = \frac{1}{2}\frac{\rho C_{p\max} R^5 \Omega^2{}_m}{\lambda_{opt}{}^3} \tag{7}$$

where C_{pmax} is the maximum power coefficient, set when λ and β are optimal values.

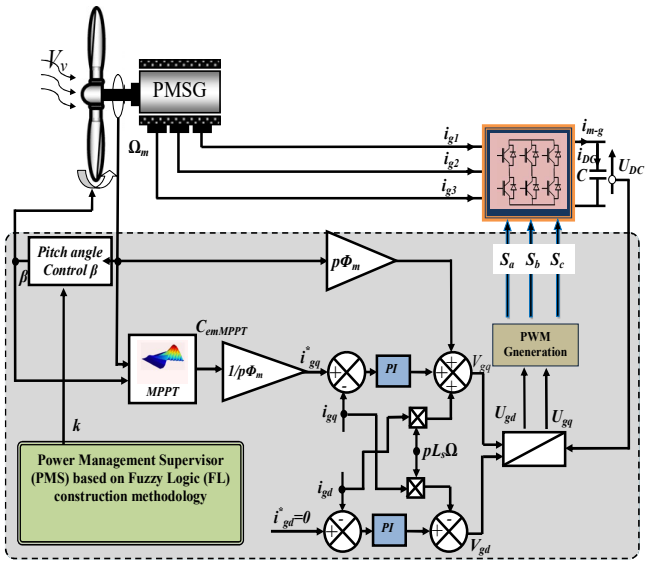

Fig. 2. Control strategy of the wind power

B. Control of the pitch angle

In normal operation, the wind turbine operates in MPPT to extract maximum of power to ensure a continuous supply of load and to participate in the system services. The overproduction of wind generated power is absorbed by the HES. But when the HES reaches its maximum SOC ''$U_{sc\text{-}max}$ (V), $SOC_{bat\text{-}max}$ (%)'' and there is overproduction of wind generator, the wind turbine operates without MPPT to produce the amount of power needed to supply the load and share in the system services. This limitation is done by the pitch angle β as follows [21]:

$$\begin{cases} \beta_{ref} = 0 \; if \; k_d = 0 \\ \beta_{ref} = \dfrac{\Delta\beta}{\Delta P}\left(P_g - P_L - P_{inj}\right) if \; k_d = 1 \end{cases} \tag{8}$$

where k_d is the degradation factor deduced by FLS.

In addition, the pitch angle β is used to limit the rotational speed, and therefore, the produced power in the case of high wind speed to avoid the damage of the turbine and the electric machine.

C. HES modeling and control

In this part, we propose to study the modeling and the control of the hybrid storage system. The considered model of the battery is constituted by a voltage source in series E_{bat} (V) with an internal resistance $R_i(\Omega)$ as follows [22]:

$$\begin{aligned} V_{bat} &= E_{bat} \pm R_i i_{bat} \\ E_{bat} &= n\left(2.15 - SOC\left(2.15 - 2\right)\right) \\ SOC &= 1 - \frac{Q_d}{C_{bat}} \end{aligned} \tag{9}$$

where E_{bat} is expressed as a function of the SOC of the battery and n the number of cells which makes up the battery.

To bring out the physical phenomena that governs the functioning of the storage, the temperature should be taken into account $\Delta T = T - 25°$. It is why we propose the model of capacity C_{bat} as a function of temperature; it gives the amount of energy Q_d that can be restored as a function of the mean discharge current i_{bat} [22]:

$$\frac{C_{bat}}{C_{10}} = \frac{1.67}{1 + 0.67\left(\dfrac{i_{bat}}{I_{10}}\right)^{0.9}}\left(1 + 0.005\Delta T\right) \tag{10}$$

With C_{10} and I_{10} are respectively the nominal capacity and current of the battery

To improve the performance of the BT storage system, other storage organs such as a supercapacitors module is introduced. A realistic modeling of a super-capacitor is composed of a series capacitance C_{ssc} (F) with a resistance $R_{ssc}(\Omega)$.

Therefore, the total resistance R_{sc} and capacitance C_{sc} of the used supercapacitors module can be defined by the following expressions [23]:

$$C_{sc} = \frac{N_p}{N_c} C_{ssc}; R_{sc} = \frac{N_c}{N_p} R_{ssc} \tag{11}$$

where N_s and N_p are the number of super-capacitor units placed respectively in series and in parallel.

The control of each storage system is done by the control of the DC / DC converters. Figure 3 schematizes this control.

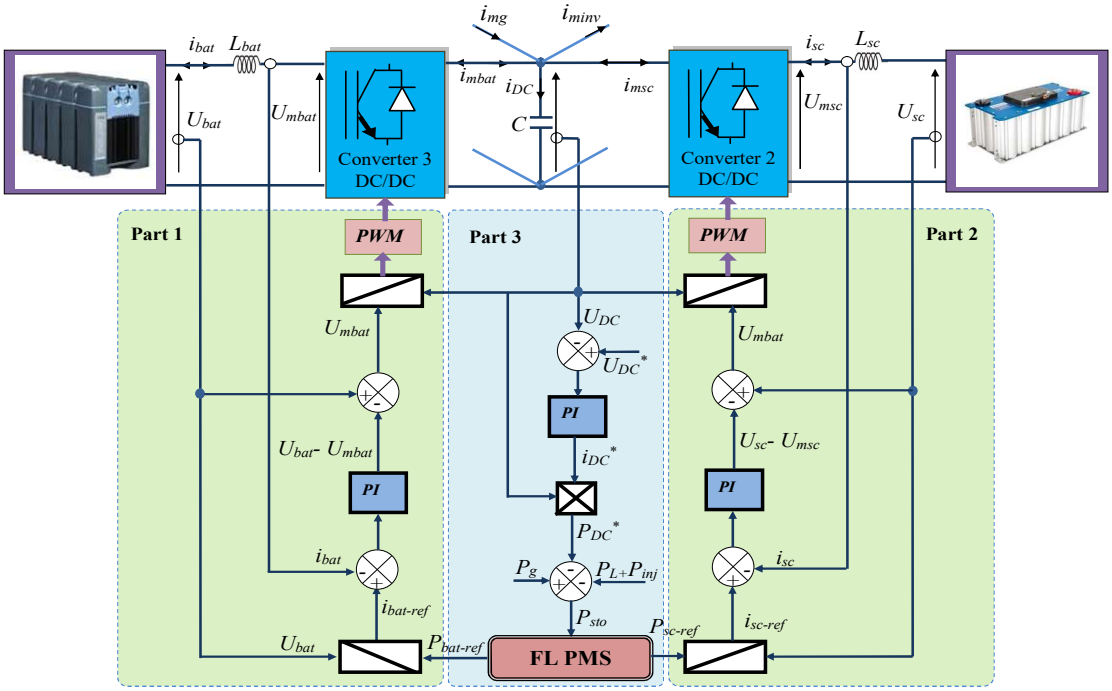

Fig. 3. DC bus and HSS control

- The part 1 of Figure 3 shows the control of charge and discharge current of battery bank by converter 3.
  - Current control: a PI regulator is used to maintain the charge or discharge current of battery bank equivalent to its reference $i_{bat\text{-}ref}$. This reference is deducted by the FLS:

$$U_{mbat} = U_{bat} - PI\left(i_{bat-ref} - i_{bat}\right) \tag{12}$$

  - Converter number 3 DC/DC control: in order to fix the direction of charging or discharging current of the BT, the BT converter is controlled by this duty ratio as follows:

$$m_{bat} = U_{mbat} / U_{DC} \tag{13}$$

- Same principle as the battery control, a PI controller is used to adjust the charge and discharge current i_{sc}(A) of SC with the reference value $i_{sc\text{-}ref}$. Subsequently, the SC converter is controlled by this duty ratio as follows (part 2 of Figure 3):

$$\begin{cases} U_{msc} = U_{sc} - PI\left(i_{sc-ref} - i_{sc}\right) \\ m_{sc} = U_{msc} / U_{DC} \end{cases} \tag{14}$$

where $i_{sc\text{-}ref}$ is deducted by the FLS.

- The third part of Figure 3 is the control of the DC bus voltage. A PI controller is put forward for maintaining the DC bus voltage U_{DC}(V) equivalent to its reference value $U_{DC\text{-}ref}$. Indeed, the DC bus control depends mainly on the proposed strategy, which consists in controlling the HES SOC and calculating its needed reference power to be absorbed or supplied.

III. Fuzzy Logic Power Management Supervisor

The objective of using fuzzy logic in this work is to manage the overall system power flow while maintaining the SOC of batteries and the level of SC voltage at their admissible intervals to ensure its safe operation. The FLS developed in this study includes three inputs and three outputs as shown in Figures 4, 5 and 6. The inputs are the difference between the produced and demanded power "P_{sto}=ΔP (W)", the SOC of batteries (SOC_{bat}), and the SC voltage (U_{sc}). The outputs are the reference power of batteries $P_{bat\text{-}ref}$, the reference power of SCs $P_{sc\text{-}ref}$, and the degradation factor to limit wind production k_d. Using the data available from these three inputs, the FLS determines the command for the regulation of the DC bus according to the different production scenarios.

A. Supervisor Structure

The objectives of energy management are detailed as follows:

- Return a smoothed power to the grid to ensure its stability.
- Deliver a continuous power corresponding to the load consumption.
- Ensure storage availability, i.e. to ensure that it does not reach its upper and lower limits.
- Keep stable the DC bus voltage.

Once the objectives of the energy supervision have been identified, it is necessary to structure the supervisor. It is therefore necessary to identify adequate inputs in order to establish the right management rules for the output set-point.

Figure 5 shows the three input variables of the power management supervisor and Figure 6 shows the three output variables. These variables are:

- The storage level or the SOC of the BT storage, it is necessary to integrate the limits of the storage system.

- The storage level of the SC module "U_{sc}", it is necessary to integrate the limits of the storage system.
- Power variations "P_{sto}(W)"
- The storage power set-point of SC "$P_{sc\text{-}ref}$(W)", following the fuzzy logic approach.
- The storage power set-point of BT "$P_{bat\text{-}ref}$(W)", following the fuzzy logic approach.
- Degradation factor of wind production "k_d".

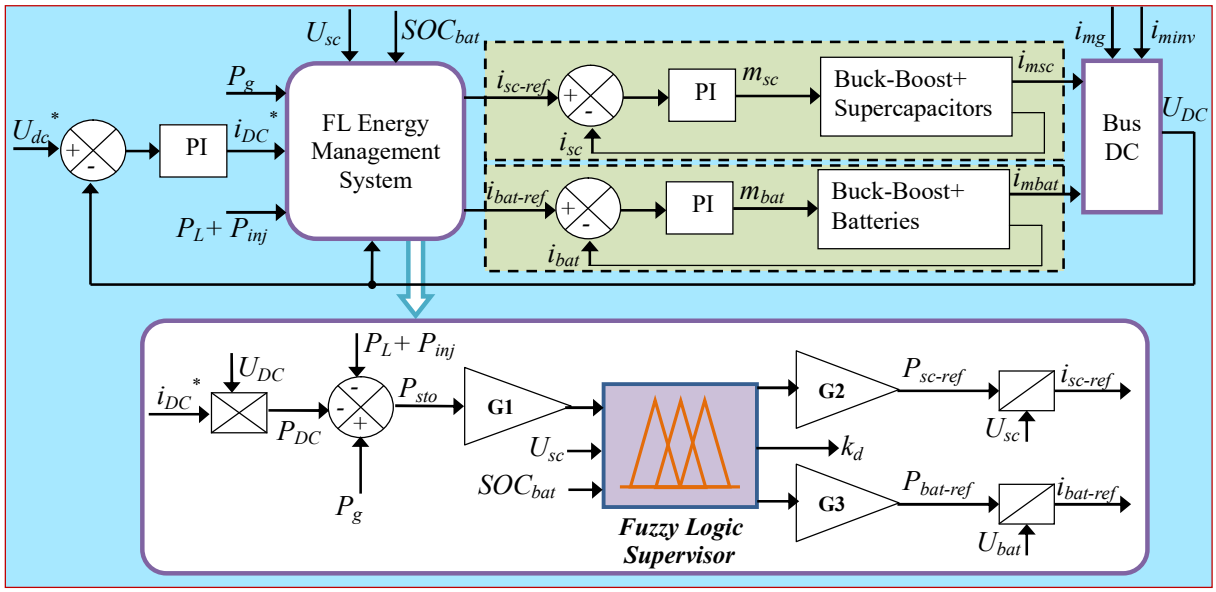

Fig. 4. Fuzzy logic supervisor strusture.

B. *Membership functions*

The determination of the membership functions for fuzzification of the input and output variable of the energy supervisor is an important phase of the fuzzy algorithm. It is necessary to define the membership functions for the three input variables "P_{sto}, SOC_{bat}, U_{sc}" and the membership functions for the three output variable values "$P_{sc\text{-}ref}$, $P_{bat\text{-}ref}$, k_d". These functions are depicted in Figure 5 and Figure 6.

The input membership functions are used as transitions between the different operating modes. For the membership function of the power variations presented in Figure 5a *"P_{sto}"*, five fuzzy sets are considered: "NB (Negative Big)", "NM (Negative Medium)", "Z (Zero)", "PM (Positive Medium)", and "PB (Positive Big)". This membership functions is estimated between 1 and -1 using a normalization gain G_1.

For SOC of each storage devices (Figure 5b, Figure 5c), the membership functions consist of three levels ("Small", "Medium", "Big"). The "Small" and "Big" sets ensure storage availability avoiding these low and high saturations. The "Medium" set is used to compensate or to absorb the difference between the generated wind power and the required power. The low level representing the SOC_{bat} is <30% (between 0 and 30%). The medium level representing the SOC_{bat} is between 30 and 90%. The high level representing the SOC_{bat} is >90% (between 90 and 100%). The low level representing the U_{sc} is <58V (between 0 and 58V). The medium level representing the U_{sc} is between 58V and 98V. The high level representing the U_{sc} is >98V.

For the membership function of the storage reference power of the BT presented in Figure 6b, three fuzzy sets are also considered:"Negative" to charge the battery, "Zero" not to request storage, and "Positive" to discharge the battery. For the membership function of the storage reference power of the SC presented in Figure 6a, five fuzzy sets are considered: "NB (Negative Big)", "NM (Negative Medium)", "Z (Zero)", "PM (Positive Medium)", and "PB (Positive Big)". These membership functions are estimated between 1 and -1 using a normalization gains G_2 and G_3 summarized in table 1.

For the membership function of the degradation factor "k_d", presented in Figure 6c, two fuzzy sets are considered: "Z" indicates that the wind generator operates in MPPT to produce the maximum power, and "P" indicates that the wind generator operates without MPPT to provide only the requested power.

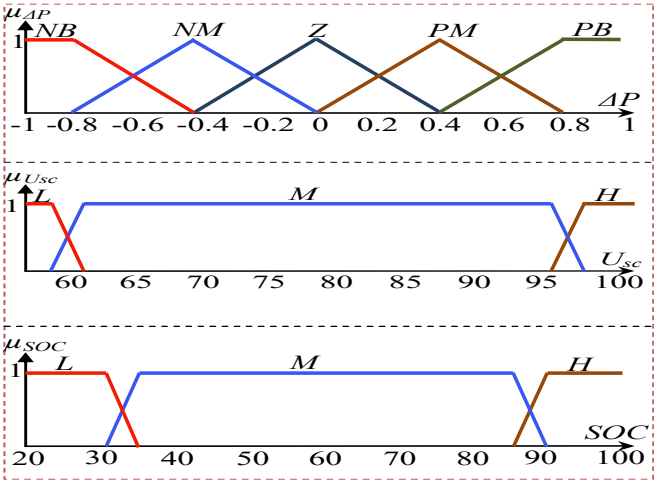

Fig. 5. Membership functions of the FLS inputs

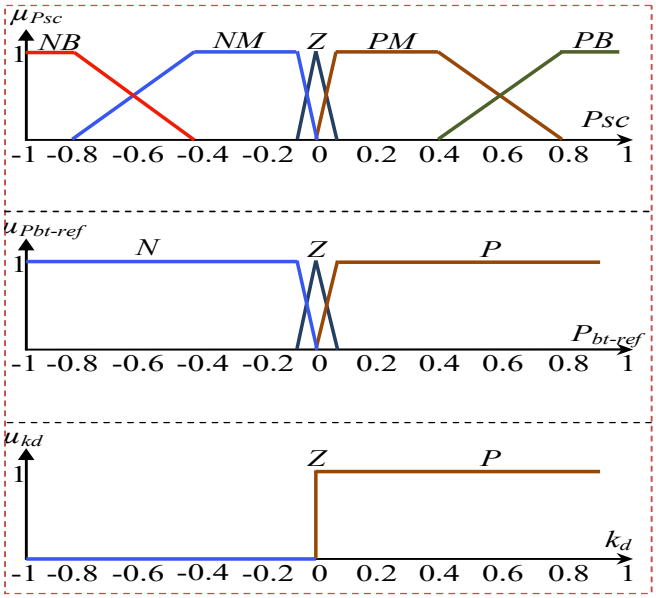

Fig. 6. Membership functions of the of the FLS outputs

The boundaries of the membership functions are determined by the knowledge of the variations plans of each function. For ease of convenience, these variations are normalized to render them in the interval [-1, 1] using normalization gains which are summarized in the following table:

TABLE I. NORMALIZATION GAINS

Gains	G_1	G_2	G_3
Value	$1 / P_{sto\text{-}max}$	$P_{sto\text{-}max}$	$P_{sto\text{-}max}$

The transition between MPPT and without MPPT operation is ensured by the degradation factor of wind production "k_d" depicted by the membership function given by Figure 6c. This factor take "0" (wind turbine operate in MPPT) when "$U_{sc}<U_{sc\text{-}max}$" and "$SOC_{bat}<SOC_{bat\text{-}max}$" and take "1" (wind turbine operate without MPPT) when "$U_{sc}\geq U_{sc\text{-}max}$" and "$SOC_{bat}\geq SOC_{bat\text{-}max}$". k_d represent the input of the aforementioned pitch angle control algorithm.

- In case of over-production "$P_g>(P_L+P_{inj})$" and the HES reaches its maximum SOC, the wind turbine in this case operates in limited mode. It provides only the power required by load and system services. This limitation is implemented by the control of the pitch angle (Figure 11a).

- In case of under-production "$P_g<(P_L+P_{inj})$" and if HES reaches its minimum SOC, the no-priority load are switched off to ensure the balance between production and consumption.

IV. SIMULATIONS RESULTS

In order to implement the methodology for control and energy supervision, the wind generator with HES ensuring continuous load supply and system services is modeled and simulated under Matlab/Simulink. The system and controllers parameters are given in the following tables.

TABLE II. PARAMETERS OF PMSG

Parameters	**value**
Stator resistance R_s	0.82 Ω
Stator inductance L_s	0.0151 H
Magnet flux Φ_m	0.4832 Wb
Nominal power	3.5 kW
Number of pole pairs p	4
Inertia J	$99*10^{-4}$ $Kg\ m^2$
Friction f	10^{-3} $N\ m\ s\ rad^{-1}$

TABLE III. PARAMETERS OF WIND TURBINE

Parameters	**value**
Nominal power	3.5 kW
Blade radius R	2 m
Optimal tip speed ratio λ_{opt}	8.15
Maximum power coefficient C_{pmax}	0.4794
Density of air ρ	1.225 $Kg\ m^3$

TABLE IV. PARAMETERS OF SC

Parameters	**value**
Capacitance C_{scc}	94 F+20-0%
Rated Voltage	78 V
DC Maximum current	50 A
SC inductor filter L_{sc}	10^{-6} H
SC series resistance R_{scc}	12.5 $m\Omega$
[U_{scmin}, U_{scmax}]	[58V, 98 V]
Leakage current	0.15 A, 75 h, 25°C.
Operating temperature	-40°C to +65°C

TABLE V. PARAMETERS OF BT

Parameters	**value**
SOC_{max}	0.9
SOC_{min}	0.3
Internal resistance R_i	0.15 Ω
Nominal voltage E_{bat0}	60 V
BT inductor filter L_{bat}	10^{-6} H

TABLE VI. PARAMETERS OF DC BUS

Parameters	**value**
Capacitance C	2200 μF
DC voltage	400 V

TABLE VII. PARAMETERS OF PI CONTROLLERS

	Parameters
PMSG controllers	$k_p = 0.82$ $k_i = 44.53$
SC controllers	$k_p = \sqrt{2} L_{sc} 2\pi f = 4.4 \times 10^{-4}$ $k_i = L_{sc} (2\pi f)^2 = 0.0987$
Battery controllers	$k_p = \sqrt{2} L_{bat} 2\pi f = 4.4 \times 10^{-4}$ $k_i = L_{bat} (2\pi f)^2 = 0.0987$
DC bus controllers	$k_p = 2\pi f \sqrt{2} C = 0.9774$ $k_i = C (2\pi f)^2 = 217.13$

To test the behavior of the system subjected to load variations and in order to test the performance of the proposed control strategy, we have used a wind profile illustrated by Figure 7a and a power requested by the loads and the system services given in Figure 7b.

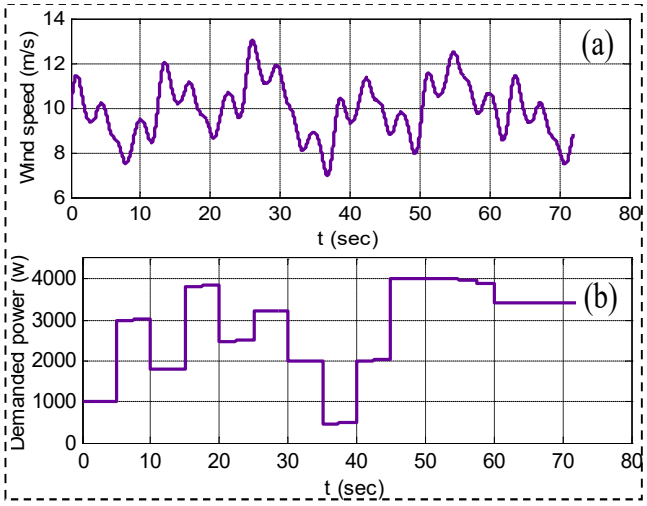

Fig. 7. (a) Wind speed, (b) demanded power

Figure 8 shows the response of the proposed control strategy to the SC. Figure 8a reproduces the evolution of the SC storage power to satisfy the production program. Figure 8b plots SC charging and discharging current that follows its set point without overtaking, showing the effectiveness of the developed control scheme. The proposed FLS avoids the deep discharge and the overcharge of the SC (Figure 8c).

Figure 9 shows the response of the proposed control strategy to the BT. Figure 9a reproduces the evolution of the BT storage power to satisfy the production program. Figure 9b shows that BT charging and discharging current follows its set point without overtaking, showing the effectiveness of the developed control scheme. The proposed FLS avoids the deep discharge and the overcharge of the BT and reduces the peak power demand, charge/discharging cycle (Figure 9c).

Figure 10 shows the dynamics of the active powers when changing the different operating modes. As shows Figure 11b, the DC-bus voltage is well regulated and the power requirements from loads and grid are well achieved.

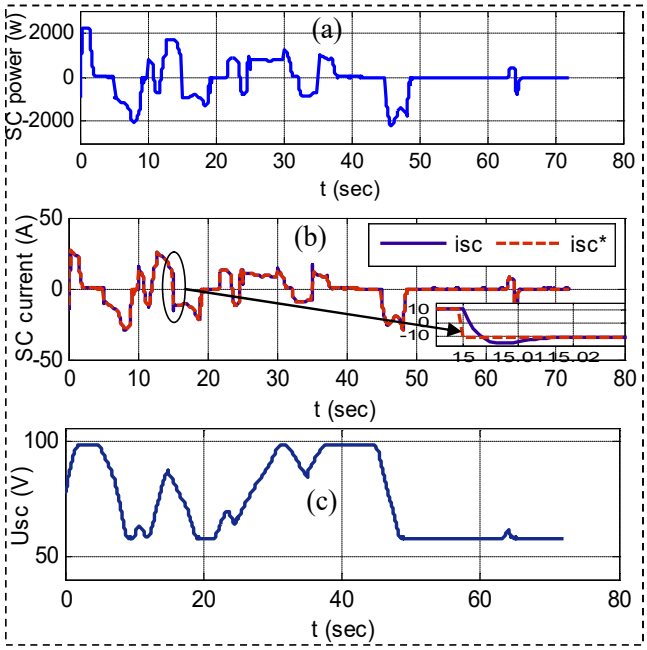

Fig. 8. (a) SC reference power, (b) SC current, (c) SC voltage

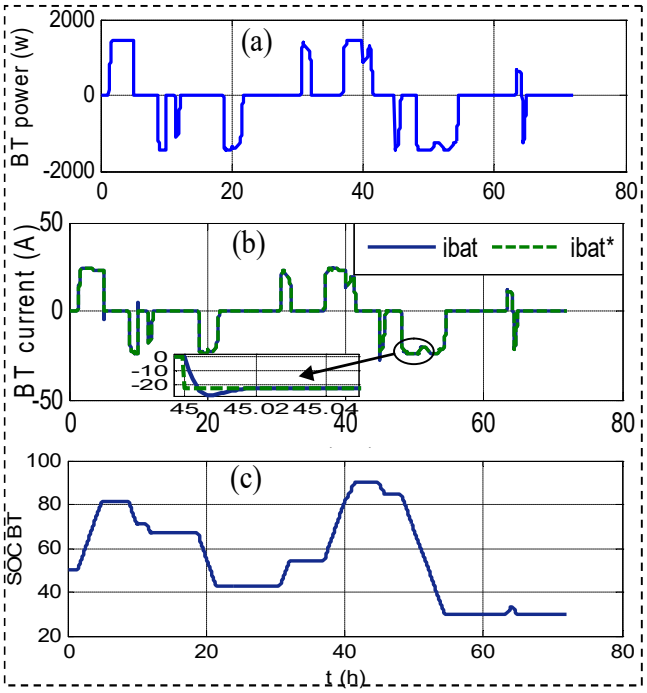

Fig. 9. (a) BT reference power, (b) BT current, (c) BT SOC

In limited operation mode (Figure 11c), the wind turbine operates without MPPT thanks to the pitch angle control (Figure 11a). It provides only the needed power for load supply and system services, since there is an excess of production and the storage system is totally charged.

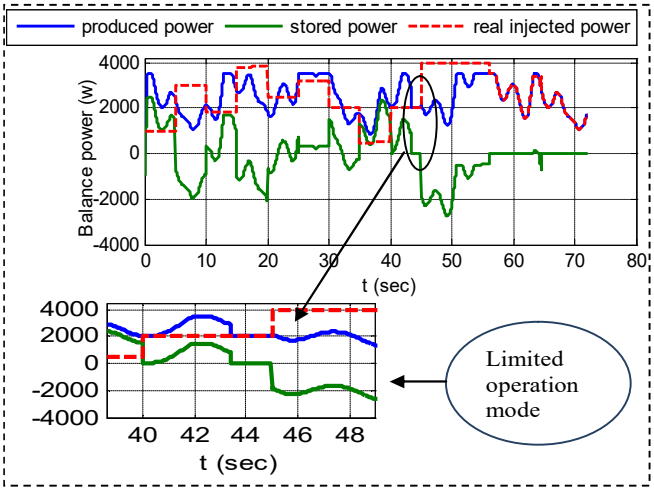

Fig. 10. Power balance to the bus voltage

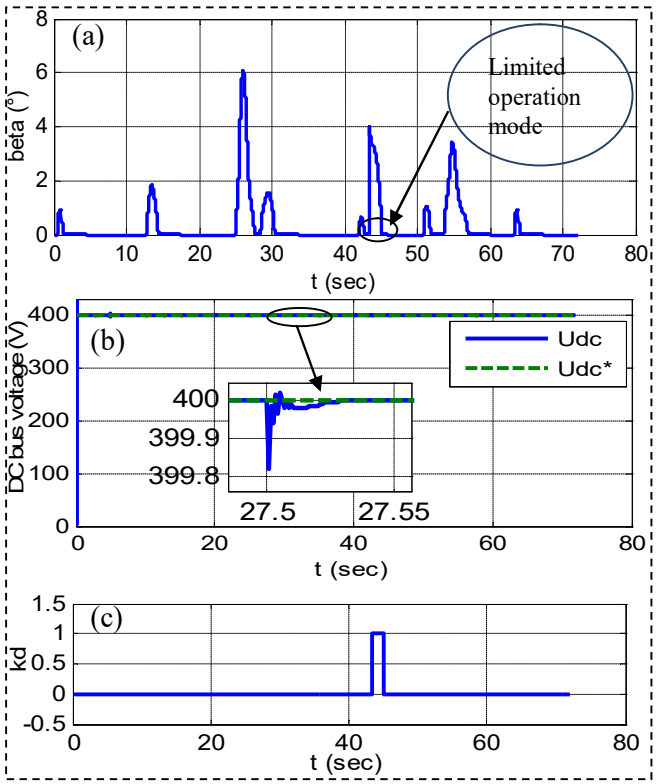

Fig. 11. (b) pitch angle β, (b) DC bus voltage, (c) K_d factor

V. CONLUSION

In this paper, a control strategy of a grid-connected wind power system with Batteries-Supercapacitor HES has been presented. This control has three main control tasks. The first one is the vector control applied to the PMSG to extract the maximum available wind power. The second one is the control of charging and discharging currents of each storage organ to maintain a stable DC voltage. The third one is the fuzzy logic supervisor which is implemented to manage the hybrid power generation to reduce the peaks in the required power of the battery and to protect the storage system against overcharge and excess discharge. Simulation results show the validity of suggested power control approach. Furthermore, an adaptive droop control based on fuzzy logic to adjust the frequency and amplitude of the grid output voltage ensuring its stability will be the objective of a future work.

REFERENCES

[1] K. Basaran , N. S. Cetin, S. Borekci, "Energy management for on-grid and off-grid wind/PV and battery hybrid systems", IET RENEWABLE POWER GENERATION, vol. 11, n°. 5, pp. 642-649, 2017.

[2] D. Lu, H. Fakham, T. Zhou, B. François, "Application of Petri nets for the energy management of a photovoltaic based power station including storage units", RENEWABLE ENERGY, vol. 35, pp. 1117–1124, 2010.

[3] C. Serir, D. Rekioua, N. Mezzai, S. Bacha, "Supervisor control and optimization of multi-sources pumping system with battery storage", INTERNATIONAL JOURNAL OF HYDROGEN ENERGY, vol. 41, n° 45, pp. 20974-20986, 2016.

[4] L. W. Chong, Y. W. Wong, R. K. Rajkumar, D. Isa, "An optimal control strategy for standalone PV system with Battery- Supercapacitor Hybrid Energy Storage System", JOURNAL OF POWER SOURCES, vol. 331, pp. 553-565, 2016.

[5] F. Bensmaine, O. Bachelier, S. Tnani, G. Champenois, E. Mouni, "LMI approach of state-feedback controller design for a STATCOM-supercapacitors energy storage system associated with a wind generation", ENERGY CONVERSION AND MANAGEMENT, vol. 96, pp. 463 – 472, 2015.

[6] R. Ahma, EP. Nowicki, "Supercapacitor energy storage system for fault ride through of a DFIG wind generation system" ENERGY CONVERSION MANAGE, vol. 59, pp. 96 – 102, 2012.

[7] N. Mendis, K. M. Muttaqi, S. Perera, "Management of Battery-Supercapacitor Hybrid Energy Storage and Synchronous Condenser for Isolated Operation of PMSG Based Variable-Speed Wind Turbine Generating Systems", IEEE TRANSACTIONS ON SMART GRID, vol. 5, no. 2, pp. 944-953, 2014.

[8] T. Ma, H. Yang, L. Lu, "Development of hybrid battery–supercapacitor energy storage for remote area renewable energy systems", APPLIED ENERGY, vol. 153, pp. 56-62, 2015.

[9] L. Xiong, W. Peng, L. P. Chiang, G. Feng, C. Fook Hoong, "Control of hybrid battery/ultra-capacitor energy storage for stand-alone photovoltaic system", ENERGY CONVERSION CONGRESS AND EXPOSITION (ECCE), 2010 IEEE, p. 336– 341, 2010.

[10] W. Jing, C. H. Lai, W. S.H. Wong, M.L. D. Wong, "Dynamic power allocation of battery-supercapacitor hybrid energy storage for standalone PV microgrid applications", SUSTAINABLE ENERGY TECHNOLOGIES AND ASSESSMENTS, vol. 22, pp. 55–64, 2017.

[11] F. Bensmaine, D. Abbes, A. Labrunie, B. Robyns, "Sizing and techno-economic analysis of a grid connected photovoltaic system with hybrid storage", UPEC 2016, Coimbra,Portugal

[12] Z. Cabrane, M. Ouassaid, M. Maaroufi, "Analysis and evaluation of battery-supercapacitor hybrid energy storage system for photovoltaic installation", INTERNATIONAL JOURNAL OF HYDROGEN ENERGY, vol. 41, n° 45, pp. 20897-20907, 2016.

[13] Y.Y. Chia, L.H. Lee, N. Shafiabady, D. Isa, "A load predictive energy management system for supercapacitor-battery hybrid energy storage system in solar application using the Support Vector Machine", APPLIED ENERGY, vol. 137 pp. 588-602, 2015.

[14] N. R. Tummuru, M. K. Mishra, S. Srinivas, "Dynamic Energy management of Hybrid Energy Storage System with High-gain PV converter", IEEE TRANSACTIONS ENERGY CONVERSION, vol. 30, pp. 150-160, 2015.

[15] A. Brka, G. Kothapalli, Y.M. Al-Abdeli, "Predictive power management strategies for stand-alone hydrogen systems: lab-scale validation", INTERNATIONAL JOURNAL OF HYDROGEN ENERGY, vol. 40, pp. 9907-9916, 2015.

[16] S.K. Kollimalla, M.K. Mishra, N.L. Narasamma, "Design and analysis of novel control strategy for Battery and Supercapacitor Storage.

[17] Y. krim D. Abbes, S. Krim, M. F. Mimouni, "Classical vector, first-order sliding mode and high-order sliding-mode control for a grid-connected variable speed wind energy conversion system: A comparative study", WIND ENGINEERING, Vol. 42, n° 1, pp.16-37, 2018.

[18] A. M. Eltamaly, H. M. Farh, "Maximum power extraction from wind energy system based on fuzzy logic control", ELECTRIC POWER SYSTEMS RESEARCH, vol. 97, pp. 144-150, 2013.

[19] F. J. Lopez, G. Kenne, F. L. Lagarrigue, "A novel online training neural network-based algorithm for wind speed estimation and adaptive control of PMSG wind turbine system for maximum power extraction", RENEWABLE ENERGY, vol. 86, pp. 38-48, 2016.

[20] B. Boukhezzar, H. Siguerdidjane, "Nonlinear control of a variable wind turbine using a two mass model", IEEE TRANSACTIONS ENERGY CONVERSION, vol. 26, pp. 149-162, 2011.

[21] J. L. Rodriguez – Amenedo, S. Arnalte et J. C. Burgos, " Automatic generation control of wind farm with variable speed wind turbine ", IEEE TRANSACTIONS ON ENERGY CONVERSION, vol. 17, n°. 2, pp. 279-284, 2002.

[22] R. Kallel, G. Boukettaya, L. Krichen, "Demand side management of household appliances in stand-alone hybrid photovoltaic system", RENEWABLE ENERGY, vol. 81, pp. 123-135, 2015.

[23] P. Thounthong, P. Tricoli, B. Davat, "Performance investigation of linear and nonlinear controls for a fuel cell/supercapacitor hybrid power plant", INTERNATIONAL JOURNAL OF ELECTRICAL POWER & ENERGY SYSTEMS, vol. 54, pp. 454-464, 2014.